Star Formation in Extremely Faint Local Volume Dwarf Galaxies

Sambit Roychowdhury
with
Jayaram N. Chengalur
Ayesha Begum, Univ of W-Madison
Igor D. Karachentsev, SAO, Russia

September 14 , 2009

Faint Irregular Galaxy GMRT Survey (FIGGS)

- Galaxies identified using the selection criteria: $M_B > -14.5$, HI Flux > 1 Jy km s^{-1}, $D_{opt} > 1'$, $\delta > -40$
- By far the largest study of HI in dwarf galaxies
- Total of 62 galaxies observed

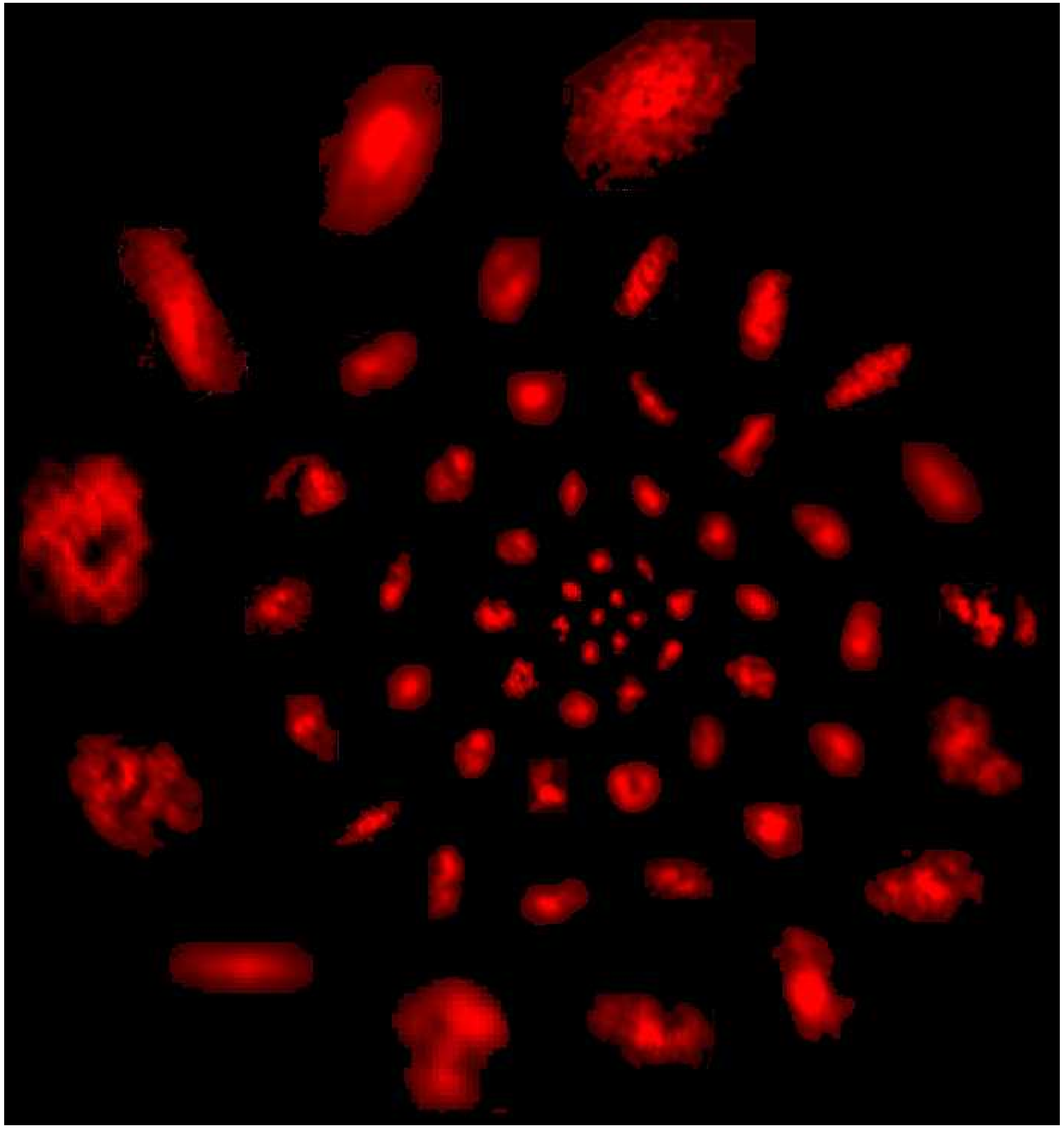

Galaxy Formation

- In heirarchical galaxy formation models small objects collapse first, and in turn merge to form large galaxies
- Simulations accurately trace only collapse and merger of dark matter halos
- Baryon physics, viz. accretion into these halos, star formation and feedback are poorly understood
- Simulation of galaxy formation necessarily use star formation 'recipes'
  - ▷ These recipes are derived from observations of nearby galaxies

Recipe one : Schmidt's Law

- Schmidt in 1959 proposed: Σ_{SFR}=A Σ_{gas}^{N}

- Kennicutt (1989, 1998) used Hα, HI and CO observations to get a Law for (optical) *disk averaged* values:

$$(2.5\pm0.7) \times 10^{-4} \left(\frac{\Sigma_{gas}}{1\ M_{\odot}\ pc^{-2}}\right)^{1.4\pm0.15}\ M_{\odot}\ yr^{-1}\ kpc^{-2}$$

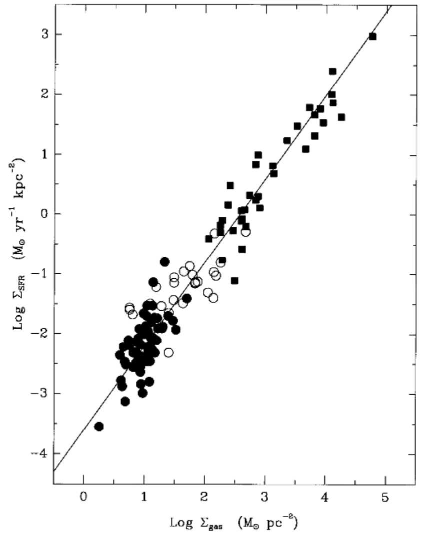

Composite star formation law for the normal disk (*filled circles*) and starburst (*squares*) samples. Open circles show the SFRs and gas densities for the centers of the normal disk galaxies. The line is a least-squares fit with index $N = 1.40$.

Recipe two : Star Formation Thresholds

- Toomre in 1964 first suggested the idea of a threshold, related to a critical density for gravitational instability in a thin rotating gaseous disk
- Skillman in 1987 proposed that star formation occurs only above a threshold column density (10^{21} atoms cm^{-2}) for a resolution of 500 pc, which may be related to a critical amount of dust sheilding required for molecular gas formation
- Kennicutt (1989), Martin & Kennicutt (2001) show SFR as traced by Hα show clear thresholds (nearby spiral galaxies)

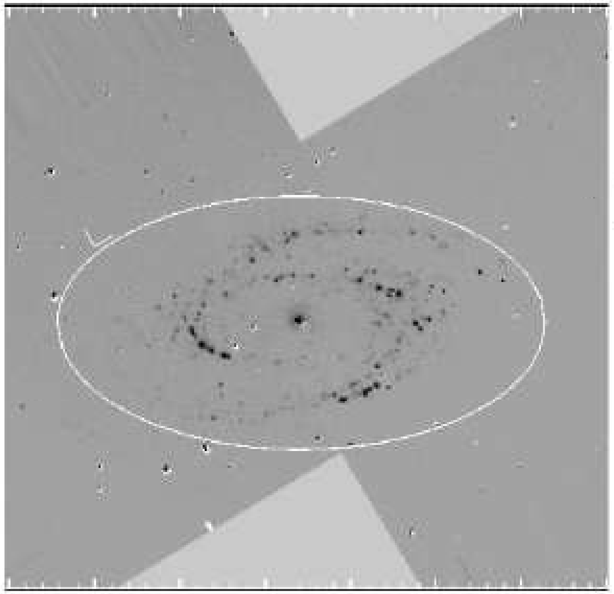

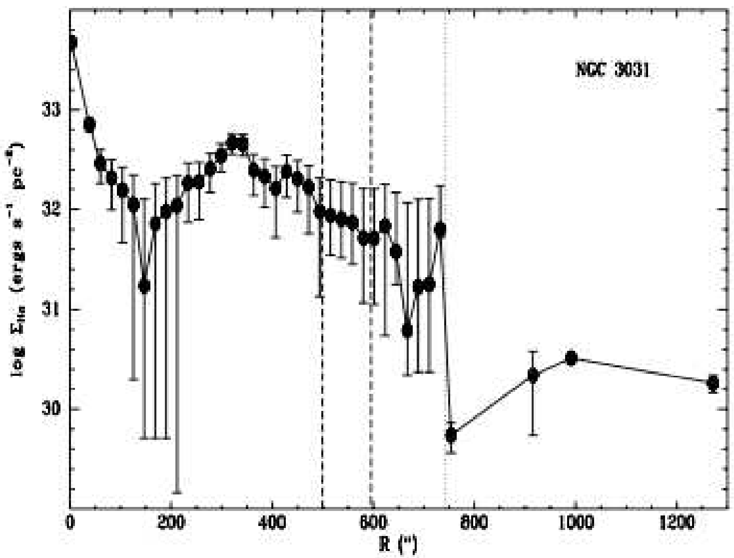

Star Formation Thresholds

- Kennicutt in 1989 combined observed Hα distributions with HI and CO data to find the threshold column density

- These thresholds represent the region where the disk goes from being dominated by molecular gas to being dominated by atomic gas

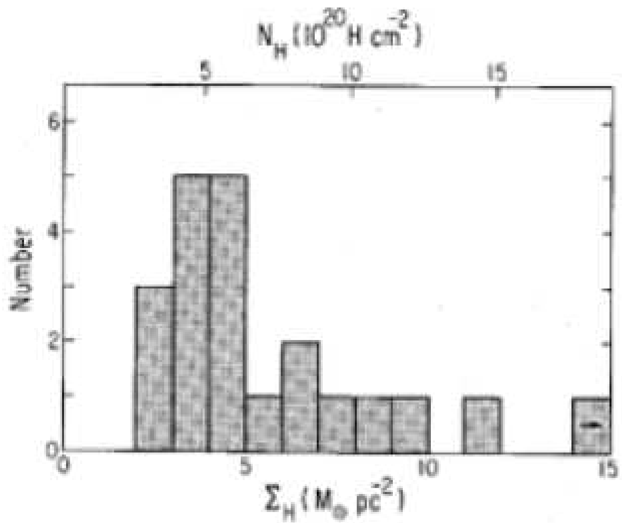

Distribution of threshold column densities in the sample. The bottom scale is in units of total (H I + H_2) hydrogen mass surface density, and the top scale is in units of hydrogen column density.

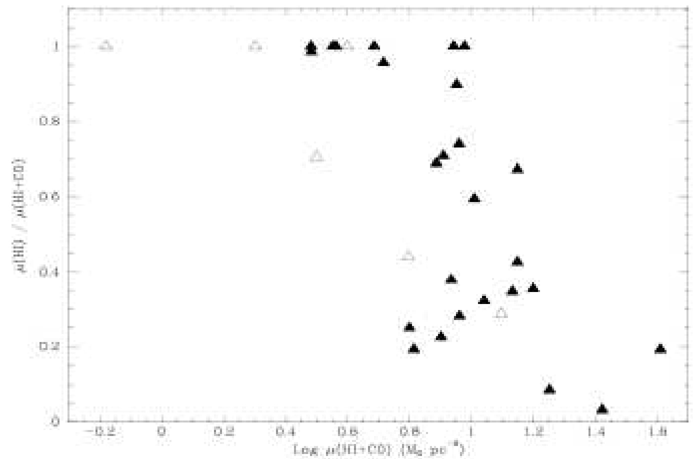

Mass fraction of atomic gas vs. total gas mass at the star formation thresholds. The subcritical disks are represented by open triangles.

Star Formation Recipes for dwarf galaxies

- All studies till now mainly looked at normal spirals or starburst galaxies

- Why should we look at dwarf galaxies?
  - ▷ Dwarf galaxies important because they lie at the beginning of the heirarchical galaxy formation scale
  - ▷ Also provide unique laboratories, low metallicity, low dust content, low pressure, etc.

- We will concentrate on a sample of local volume dwarf galaxies

DATA

- HI data taken from Faint Irregular Galaxies GMRT Survey (FIGGS), median $M_B \approx$ -13.0, median mass $\approx 3 \times 10^7$ $M_\odot$ (Begum et al., 2008)

- UV data obtained from GALEX public releases, last release in June 2008

  - ▷ circular images of the sky with 1.2° diameter and 5″ resolution

  - ▷ FUV band (1350 Å to 1750 Å) data used

- From the FIGGS sample we could find 23 galaxies which had GALEX data, and for which we could reach linear resolutions of $\approx$ 400 pc

The Sample

Galaxy	α (J2000) (h m s)	δ (J2000) (° ′ ″)	M_B (mag)	Dist (Mpc)	Group
And IV	00 42 32.30	+40 34 19	−12.23	6.3	I342
UGC 685	01 07 22.30	+16 41 02	−14.31	4.5	Field
KK 14	01 44 42.70	+27 17 16	−12.13	7.2	N672
UGC 3755	07 13 51.80	+10 31 19	−14.90	6.96	Field
DDO 43	07 28 17.20	+40 46 13	−14.75	7.8	Field
KK 65	07 42 31.20	+16 33 40	−14.29	7.62	Field
UGC 4459	08 34 06.50	+66 10 45	−13.37	3.56	M81
UGC 5186	09 42 59.80	+33 15 52	−12.98	6.9	Field
UGC 5209	09 45 04.20	+32 14 18	−13.15	6.7	Field
UGC 6456	11 28 00.60	+78 59 29	−14.03	4.3	M81
UGC 6541	11 33 29.10	+49 14 17	−13.71	3.9	CVn I
NGC 3741	11 36 06.40	+45 17 07	−13.13	3.0	CVn I
DDO 99	11 50 53.00	+38 52 50	−13.52	2.6	CVn I
E321-014	12 13 49.60	−38 13 15	−12.70	3.2	Cen A
KK 144	12 25 27.90	+28 28 57	−12.59	6.3	CVn I
DDO 125	12 27 41.80	+43 29 38	−14.16	2.5	CVn I
UGC 7605	12 28 39.00	+35 43 05	−13.53	4.43	CVn I
UGC 8215	13 08 03.60	+46 49 41	−12.26	4.5	CVn I
DDO 167	13 13 22.80	+46 19 11	−12.70	4.2	CVn I
DDO 181	13 39 53.80	+40 44 21	−13.03	3.1	CVn I
DDO 183	13 50 51.10	+38 01 16	−13.17	3.24	CVn I
UGC 8833	13 54 48.70	+35 50 15	−12.42	3.2	CVn I
KKH 98	23 45 34.00	+38 43 04	−10.78	2.5	Field

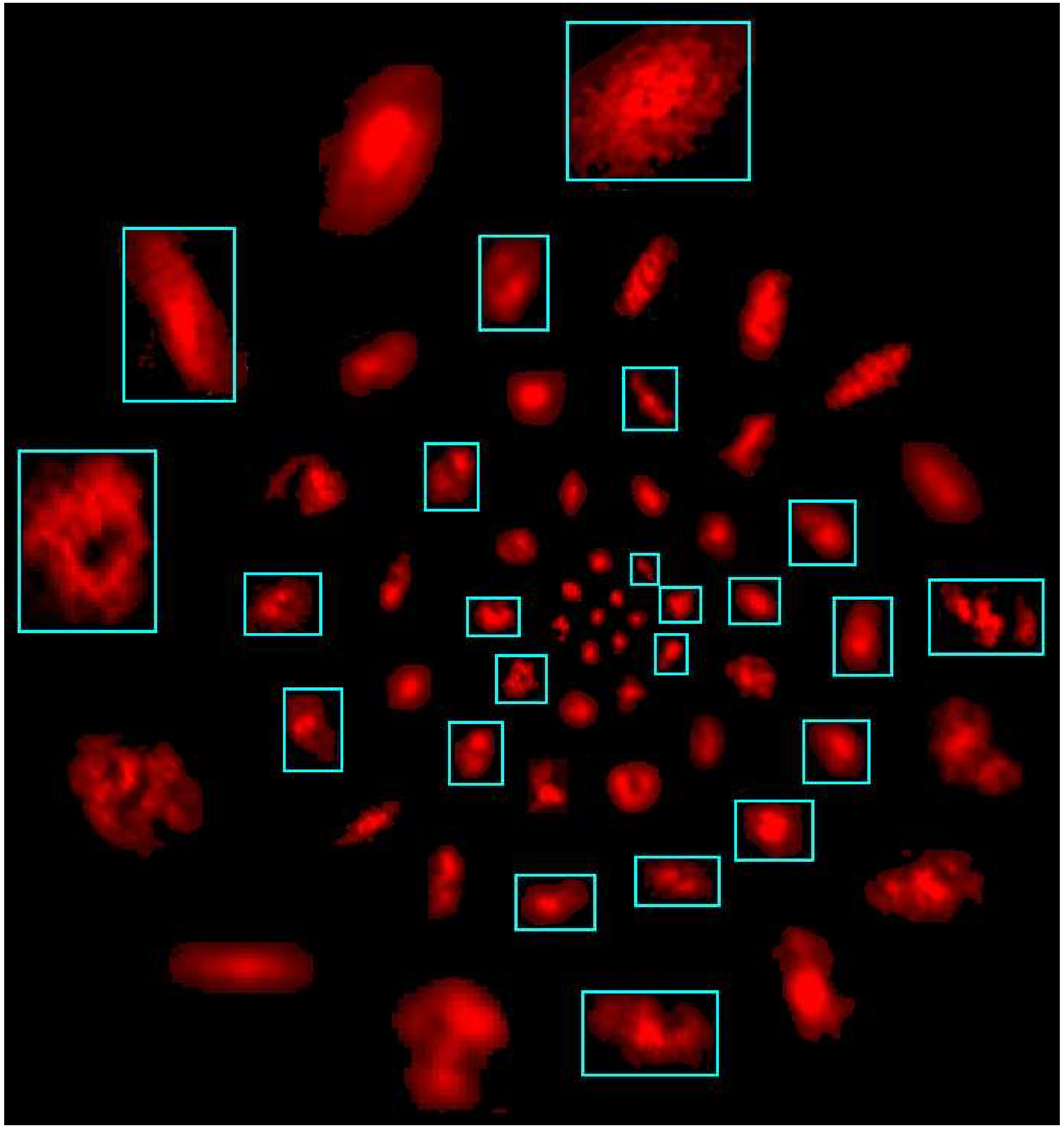

DATA ANALYSIS

- Tasks in Classic AIPS used to reduce data

- For HI data, data cubes of resolution $\approx$ 400 pc were made from available continuum subtracted data using IMAGR

- Background subtracted FUV maps were aligned to their corresponding moment 0 maps using HGEOM, then smoothed to required resolution using SMOTH (or CONVL)

DATA ANALYSIS

Galaxy	synthesised beam (arcsec^2)	synthesised beam (pc^2)	Noise (mJy)	Flux cutoff (mJy)
And IV	13,86×12.71	423×388	1.4	2.5
UGC 685	16.81×15.98	367×349	1.8	3.5
KK 14	13.38×09.99	467×349	2.1	3.3
UGC 3755	11.81×11.07	398×374	1.9	2.0
DDO 43	11.67×9.53	441×360	1.5	2.5
KK 65	11.49×10.26	424×379	1.3	2.0
UGC 4459	24.86×21.09	429×364	1.6	3.0
UGC 5186	12.14×10.48	406×351	1.1	1.5
UGC 5209	12.80×10.70	416×348	2.0	3.5
UGC 6456	19.38×17.01	404×355	2.9	5.5
UGC 6541	22.68×21.36	429×404	3.4	7.0
NGC 3741	28.21×27.02	410×393	2.4	5.0
DDO 99	33.26×29.41	419×371	2.9	6.0
E321-014	29.88×21.68	464×336	2.5	5.5
KK 144	15.99×10.28	488×314	2.0	3.5
DDO 125	34.78×30.04	422×364	3.4	6.0
UGC 7605	22.28×14.84	479×319	1.7	3.0
UGC 8215	19.02×17.94	415×391	2.4	4.0
DDO 167	20.66×18.83	421×383	3.4	6.5
DDO 181	29.77×25.16	447×378	2.7	5.5
DDO 183	27.42×24.46	431×384	2.2	4.0
UGC 8833	26.44×25.17	410×390	2.6	5.0
KKH 98	34.46×31.63	418×383	2.4	5.5

DATA ANALYSIS

- FUV data converted to SFR using

$$m_{GALEX} = -2.5 \log(cps)$$
$$m_{AB} = m_{GALEX} + 18.82$$

$$SFR(M_{\odot}\ year^{-1}) = 1.4 \times 10^{-28} L_{\nu}(ergs\ s^{-1}\ Hz^{-1})$$

(from Kennicutt 1998a, valid within the range 1250-2500 Å)

- HI data converted to column density using

$$N_H = 1.8224 \times 10^{18} \int_{-\infty}^{\infty} T_b(\nu)[K]\, dv[Km\ s^{-1}]$$

where $\frac{2kT_b}{\lambda^2} = B_{\nu}$

for Disk Averaged Values

- The task BLSUM was used to extract the total flux density over the optical disk from the respective data cubes, which was then converted to column density

- The task BLSUM was used to get the average FUV flux in the smoothed images coming from the elliptical region having ellipticity same as the optical disk, but having Σ_{SFR} equal to $1.85 \times 10^{-4} M_{\odot} yr^{-1} kpc^{-2}$ at it's edge. This Σ_{SFR} is the average UV flux at the edge of the optical disk for the four galaxies in our sample for which only Holmberg radius was available.

Global Kennicutt-Schmidt law

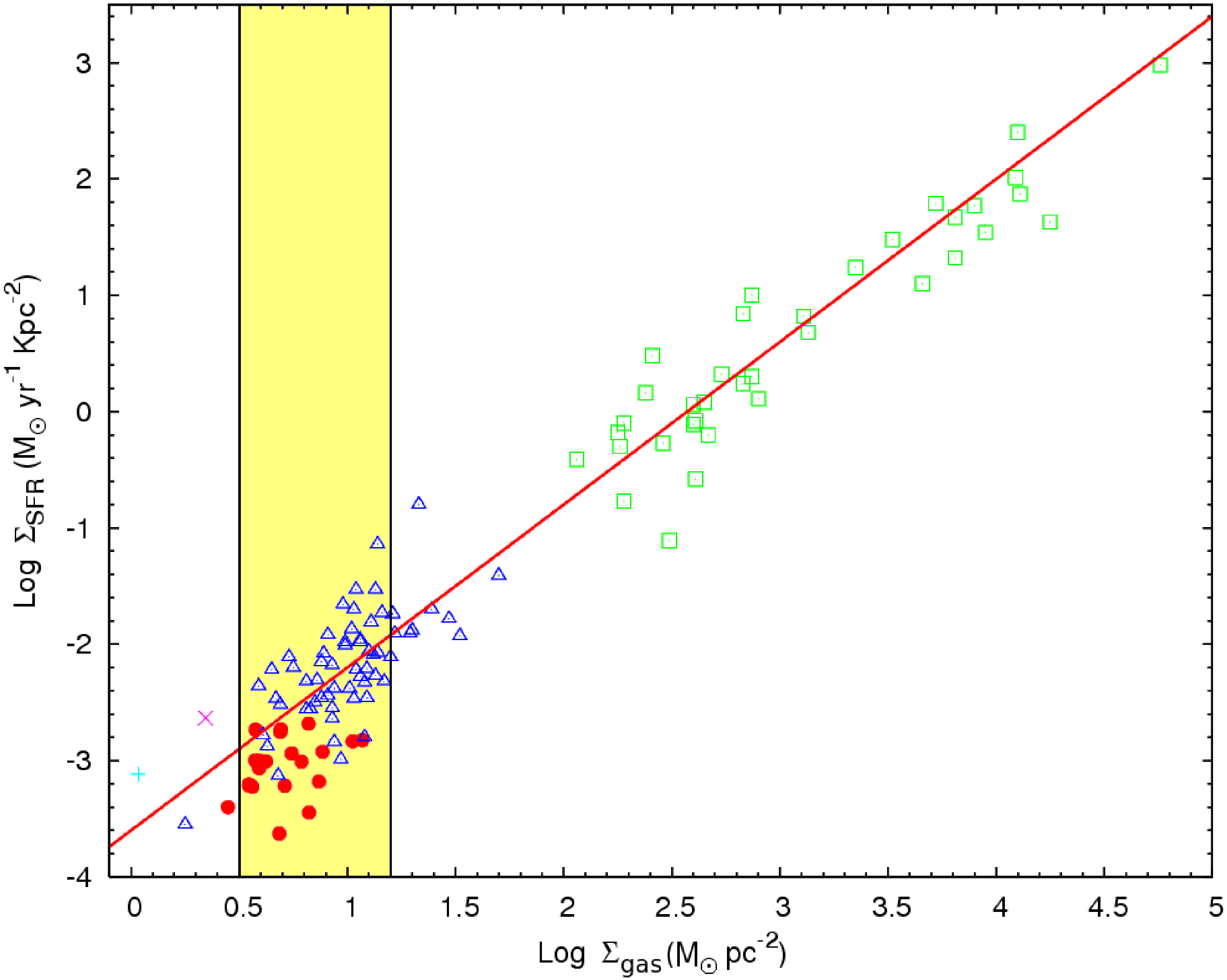

Kennicutt-Schmidt law for spirals and dwarfs

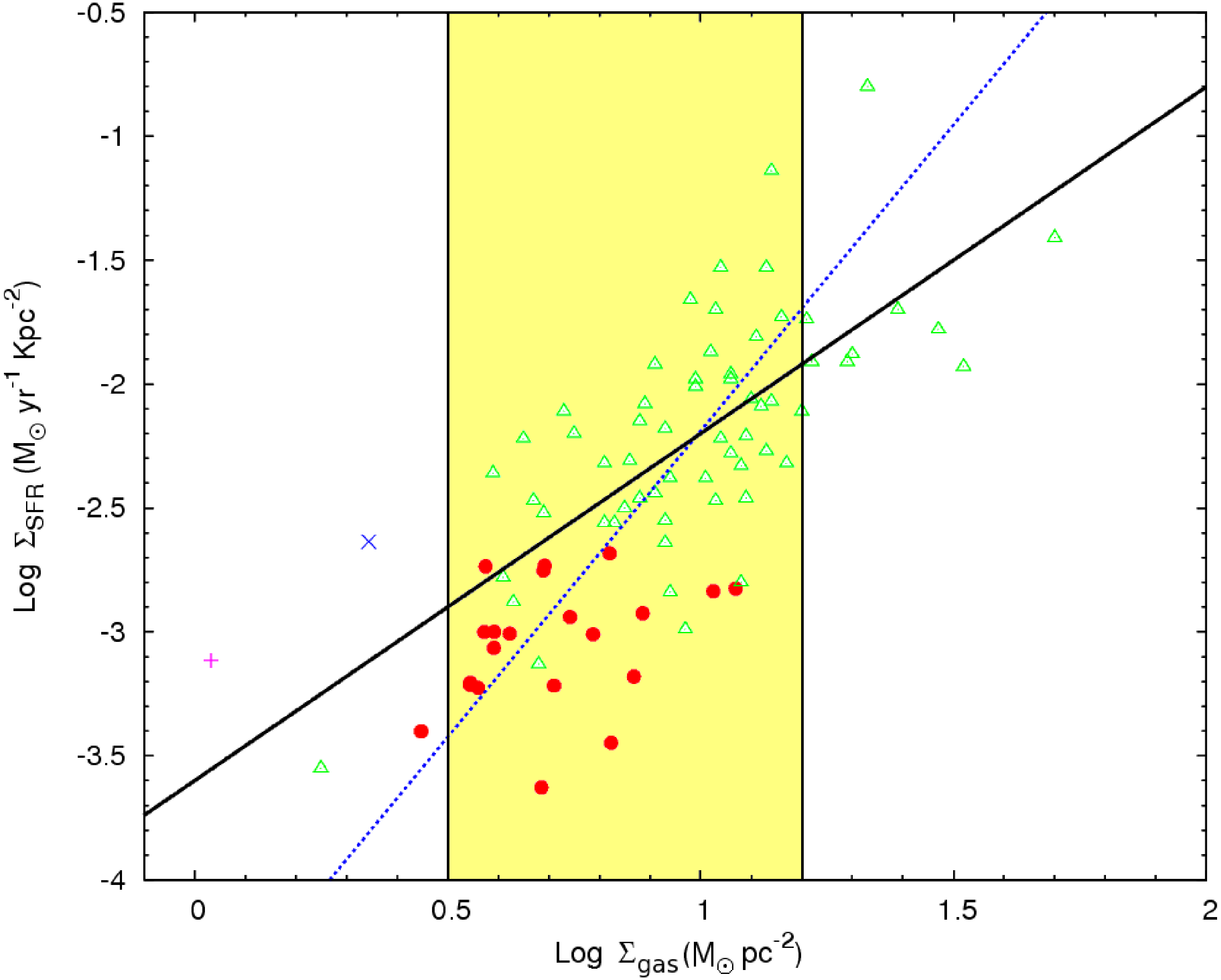

for Pixel by Pixel Comparison

- Moment 0 maps constructed using MOMNT
- Data over each 'pixel' (as shown below) averaged over

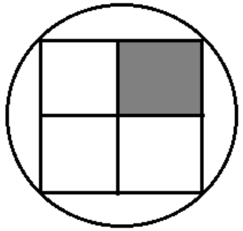

- For 10 galaxies, a similar procedure as described before was followed to get pixel by pixel comparisons at linear resolutions of ≈ 200 pc

Galaxy	synthesised beam (arcsec^2)	synthesised beam (pc^2)	Noise (mJy)	Flux cutoff (mJy)
UGC 4459	12.76×10.47	220×181	1.4	2.5
UGC 6541	11.71×9.50	221×180	2.0	3.5
NGC 3741	14.94×12.32	217×179	1.8	3.5
DDO 99	16.37×14.84	206×187	2.6	5.0
E321-014	16.03×10.09	249×157	2.0	3.0
DDO 125	20.64×13.19	250×160	2.7	3.5
DDO 181	14.33×12.22	215×184	2.2	3.5
DDO 183	14.17×10.90	223×171	1.7	2.5
UGC 8833	16.44×9.21	255×143	1.6	3.0
KKH 98	18.76×14.39	227×174	2.4	3.5

Pixel by Pixel Comparison

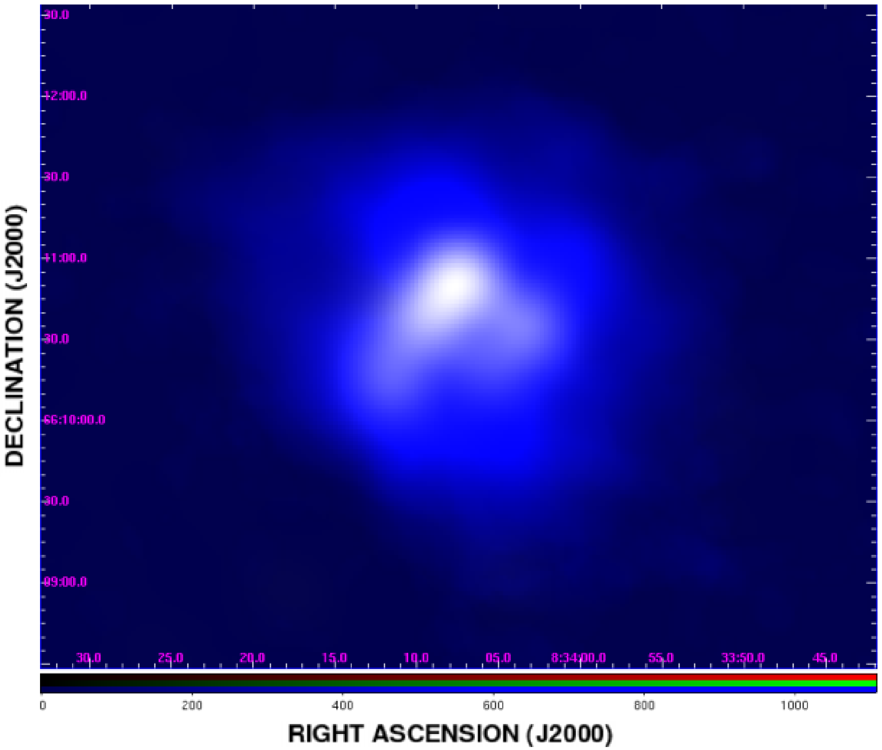

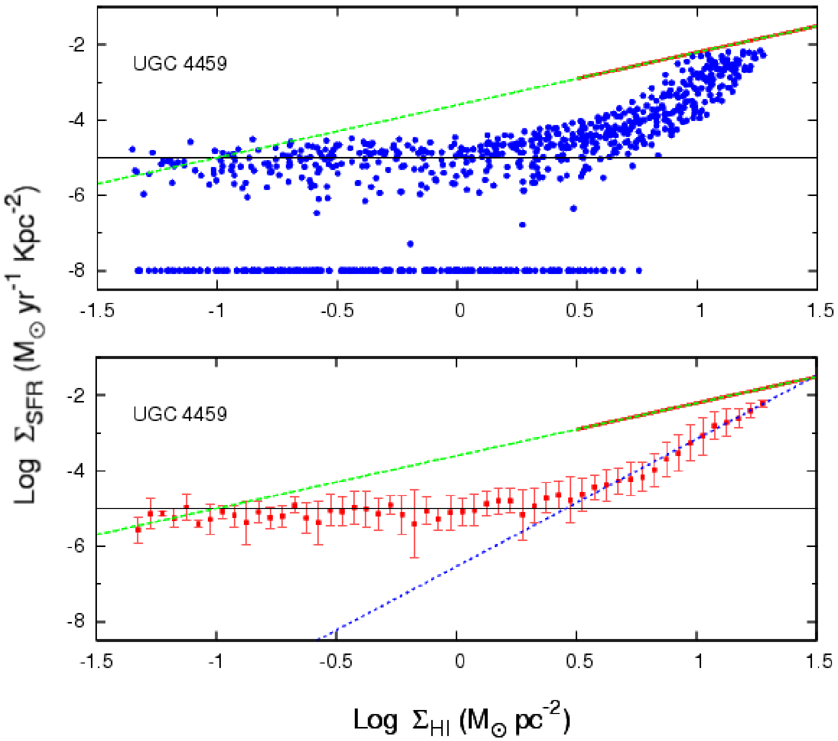

Pixel by Pixel Comparison

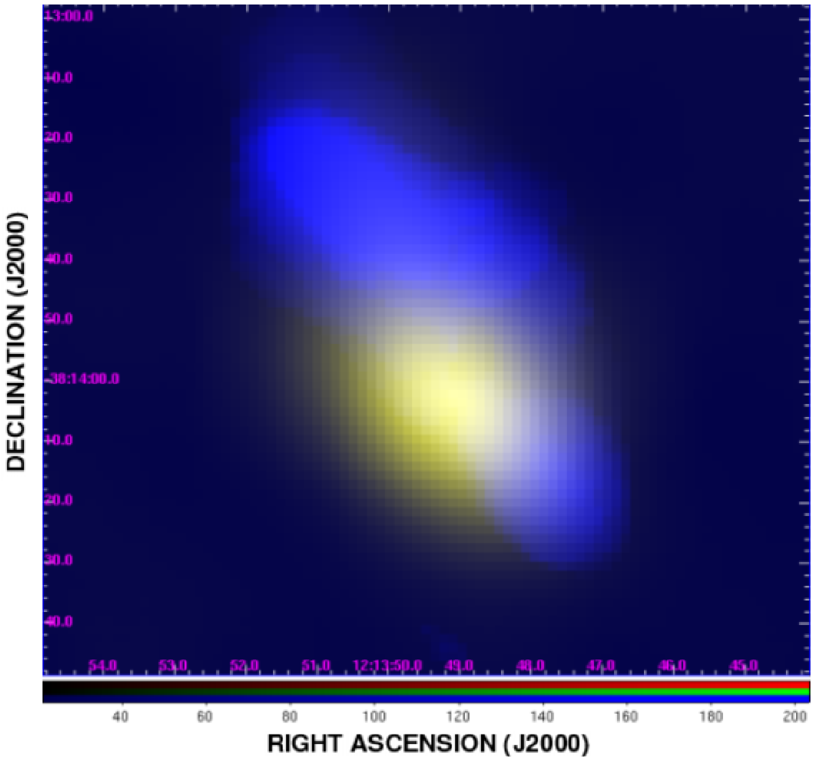

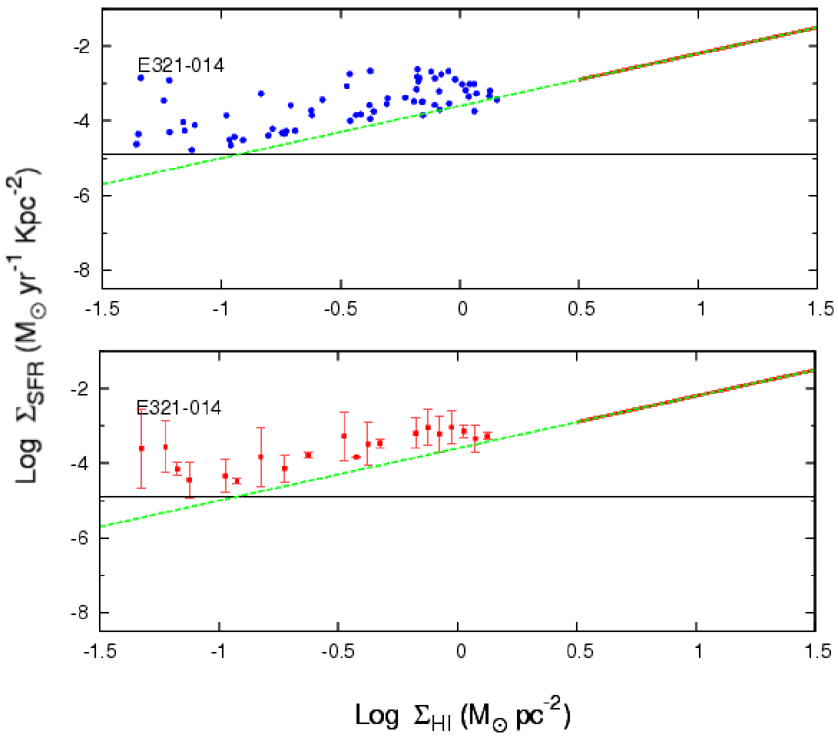

Pixel by Pixel Comparison

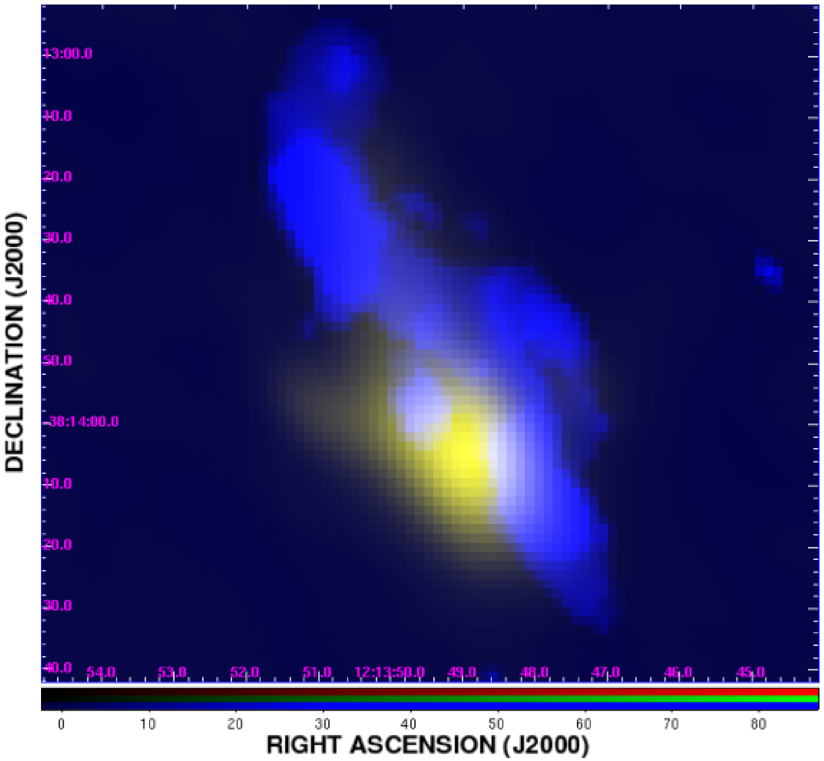

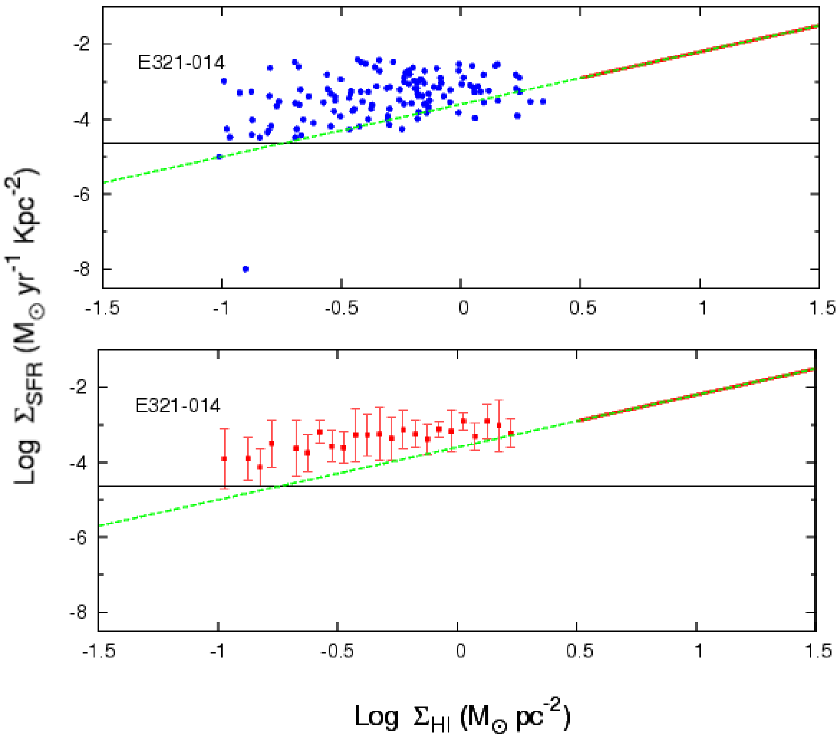

The derived quantities, for 400 pc resolution

Galaxy	Total M_{HI} [10^6 $M_\odot$]	sensitivity limit of FUV [log($M_\odot$ yr^{-1} Kpc^{-2})]	power law index	coefficient in log	range of fit
And IV	205.19	-4.89	2.3±0.1	-5.4±0.1	[0.225,0.925]
UGC 685	56.15	-4.91	1.45±0.06	-4.5±0.8	[-0.275,1.475]
KK 14	21.93	-4.04			
UGC 3755	41.30	-3.87	2.6±0.1	-4.9±0.1	[0.425,1.125]
DDO 43	203.02	-4.12			
KK 65	34.38	-4.14	1.7±0.1	-4.4±0.1	[0.175,1.025]
UGC 4459	64.2	-5.0	3.38±0.08	-6.54±0.09	[0.475,1.275]
UGC 5186	15.66	-4.53	1.62±0.07	-3.98±0.03	[-0.275,0.825]
UGC 5209	21.10	-4.36			
UGC 6456	43.89	-4.60	1.8±0.1	-3.70±0.06	[-0.475,0.925]
UGC 6541	9.65	-4.61			
NGC 3741	130.0	-5.35	4.4±0.2	-6.3±0.2	[0.225,0.875]
DDO 99	52.42	-5.15	2.6±0.2	-4.8±0.1	[-0.125,0.875]
E321-014	3.13	-4.90			
KK 144	81.15	-4.57	1.46±0.06	-4.50±0.06	[-0.025,1.025]
DDO 125	31.87	-5.37	2.41±0.07	-4.66±0.04	[-0.275,0.775]
UGC 7605	22.29	-5.13	1.60±0.06	-3.69±0.05	[-0.875,0.975]
UGC 8215	21.41	-5.26	3.1±0.2	-5.7±0.1	[0.175,0.825]
DDO 167	14.51	-5.19	1.8±0.2	-3.8±0.1	[-0.675,0.875]
DDO 181	27.55	-5.38	2.6±0.1	-4.83±0.05	[-0.175,0.725]
DDO 183	25.90	-5.58	1.88±0.04	-4.26±0.03	[-0.675,0.725]
UGC 8833	15.16	-5.06	2.25±0.09	-5.08±0.07	[-0.075,1.075]
KKH 98	6.46	-4.79	3.1±0.1	-4.74±0.04	[0.025,0.475]

The derived quantities, for 200 pc resolution

Galaxy	Total M_{HI} [10^6 $M_\odot$]	sensitivity limit of FUV [log($M_\odot$ yr^{-1} Kpc^{-2})]	power law index	coefficient in log	range of fit
UGC 4459	64.2	-4.75	2.75±0.09	-5.98±0.09	[0.475,1.375]
UGC 6541	9.65	-4.27			
NGC 3741	130.0	-5.20	3.9±0.1	-6.1±0.1	[0.225,1.025]
DDO 99	52.42	-4.93			
E321-014	3.13	-4.64			
DDO 125	31.87	-5.17	1.50±0.04	-4.26±0.02	[-0.575,0.925]
DDO 181	27.55	-5.18			
DDO 183	25.90	-5.31	2.6±0.1	-5.26±0.09	[0.025,0.975]
UGC 8833	15.16	-4.81	1.37±0.03	-4.38±0.03	[-0.275,1.225]
KKH 98	6.46	-4.59			

Simulation

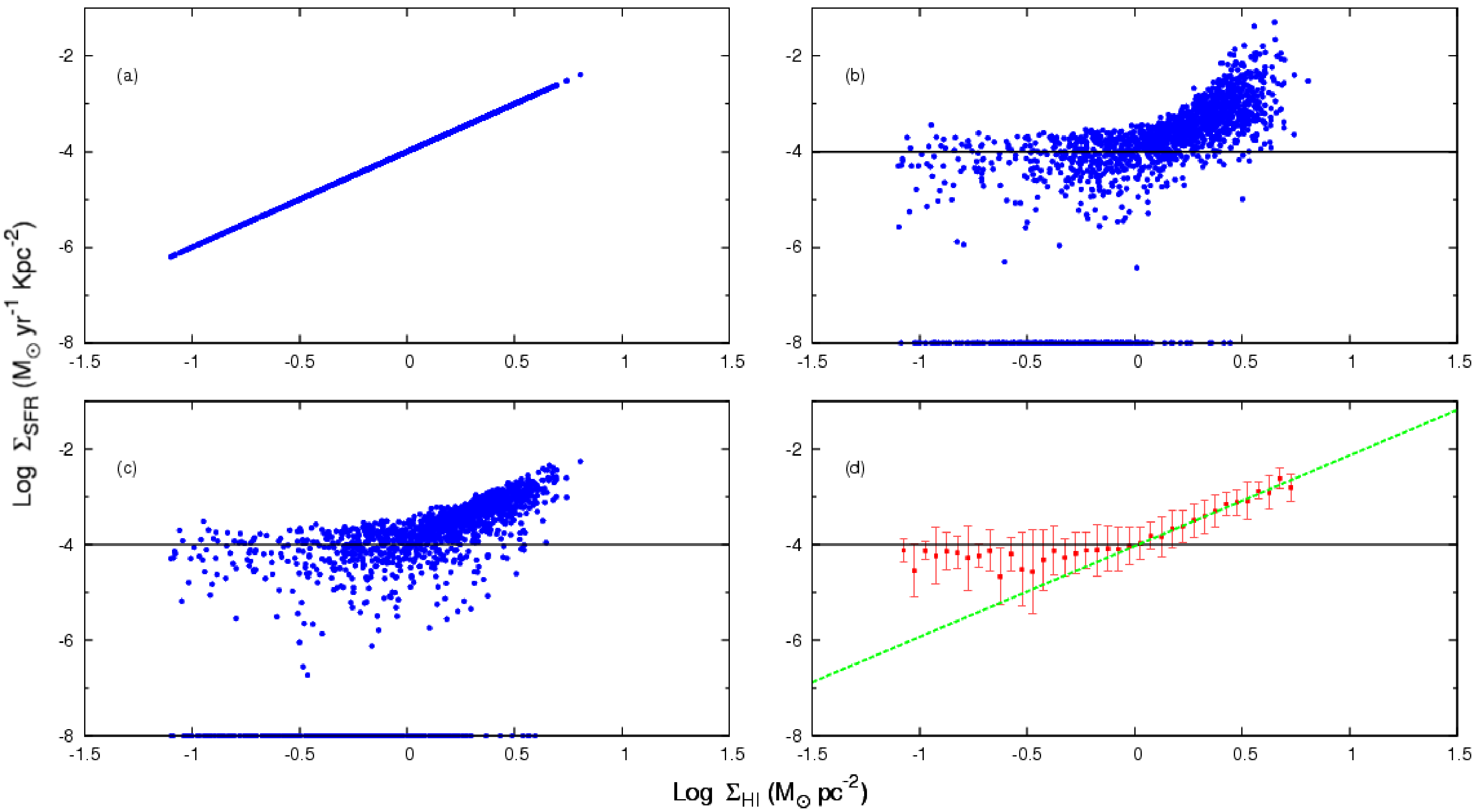

(a)
(b)
(c)
(d)
-2
-4
-6
-8
-1.5
-1
-0.5
0
0.5
1
1.5
Log Σ_{SFR} ($M_\odot$ yr^{-1} Kpc^{-2})
Log Σ_{HI} ($M_\odot$ pc^{-2})

Summary

- The globally averaged gas density in our sample galaxies lies below most estimates of the star formation rate, and the observed $\Sigma_{\rm SFR}$ is also lower than that estimated from the Kennicutt-Schmidt relation

- The data is better fit by the steeper slope found for the spirals only sample by Kennicutt (1998)

- For most (18/23) galaxies $\Sigma_{\rm SFR}$ can be parametrized to have a power law dependence on $\Sigma_{\rm gas}$ when both parameters are measured on 400 pc scales, however the coefficient and index of the power law varies substantially from galaxy to galaxy

- The index of the power law is in general steeper than the value of 1.4 for the Kennicutt (1998) relation. The observed SFR rate is in general lower than that predicted by this relation, with the discrepancy decreasing at the highest gas column densities

- At 400 pc resolution the SFR continues to fall smoothly until one reaches the sensitivity limit of our observations, and there is no evidence for a “threshold density” below which star formation is completely cut off

- At 200 pc resolution, offsets between the sites of current star formation and the locations where the gas density peaks become more pronounced, and the SFR can be parametrized as having a power law dependence on the gas density for only 5/10 galaxies

- For the majority of these galaxies (4/5) the power law index measured at 200 pc is flatter than that measured at 400 pc

Caveats

- Assumptions:
  - ⋆ Very little molecular gas present
  - ⋆ The stars have solar metallicity and Salpeter IMF
  - ⋆ The galaxy has had continuous star formation over time-scales of 10^8 years or longer
  - ⋆ Internal and external dust attenuation has been correctly accounted for

Caveats

- Effect of taking molecular gas into account shown by brown arrow
- Effect of taking sub-solar metallicities shown by blue arrow

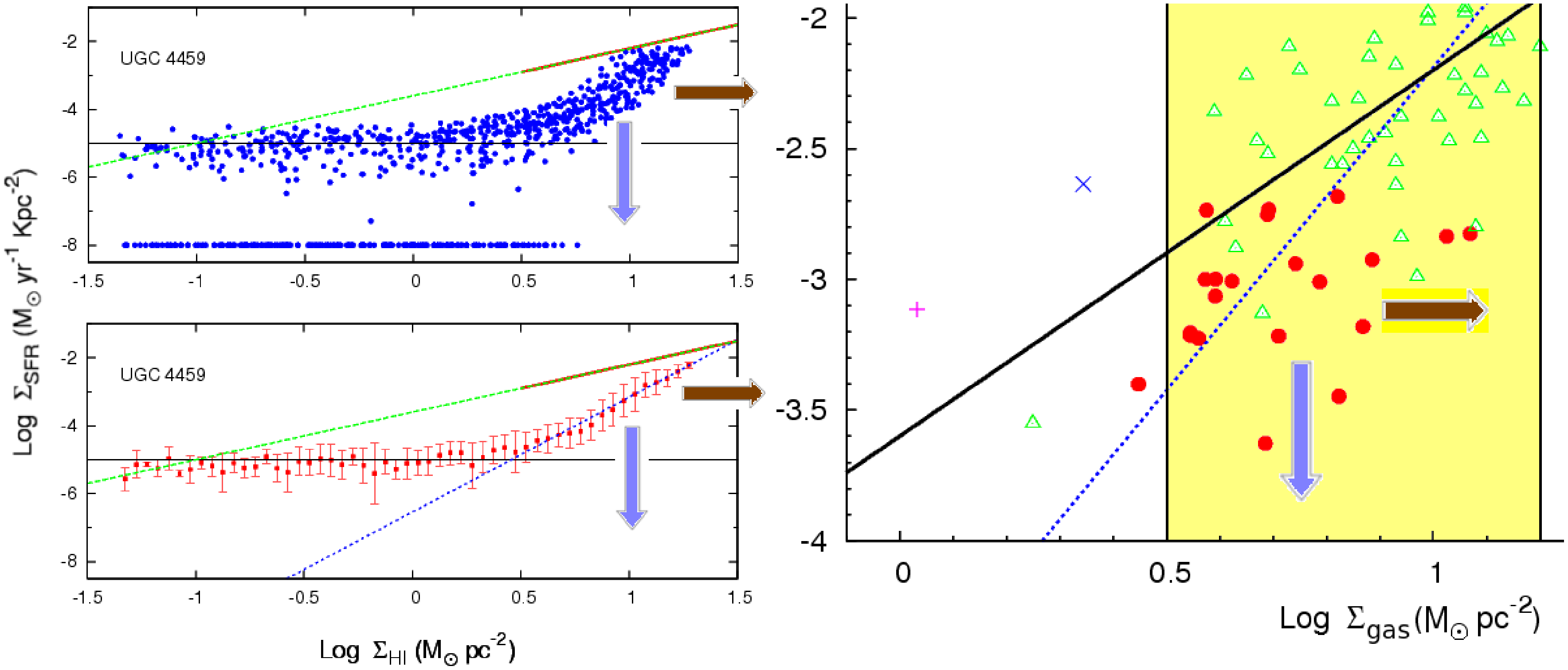

Caveats

- Truncating the IMF at the high mass end, presence of unaccounted for dust, or if the galaxy has not undergone star formation in the recent past, would affect the results as shown by the blue arrow
- Brown arrow shows how the results will change if the star formation is dominated by a recent star burst

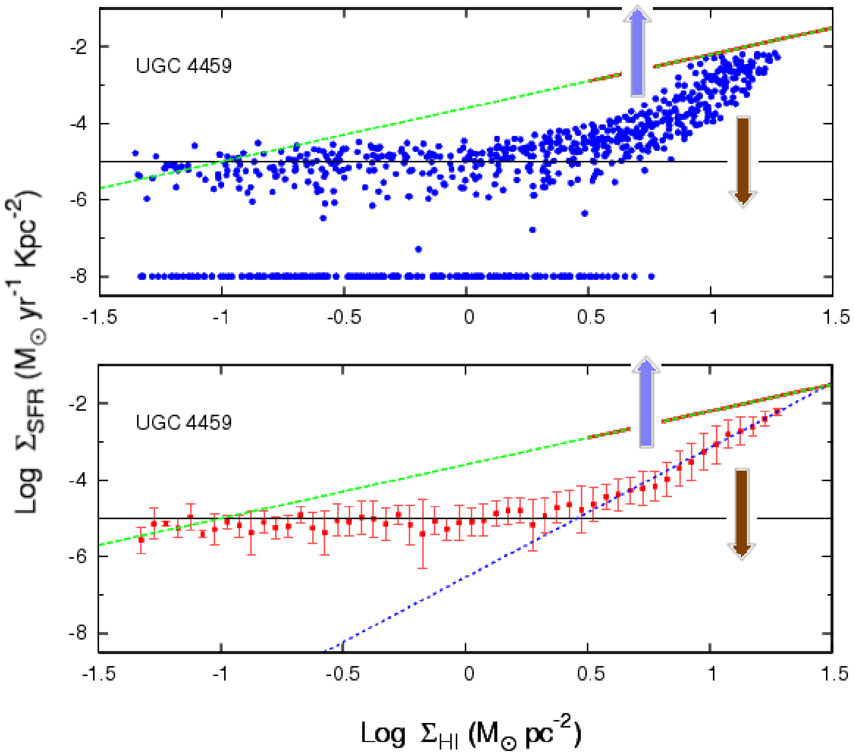

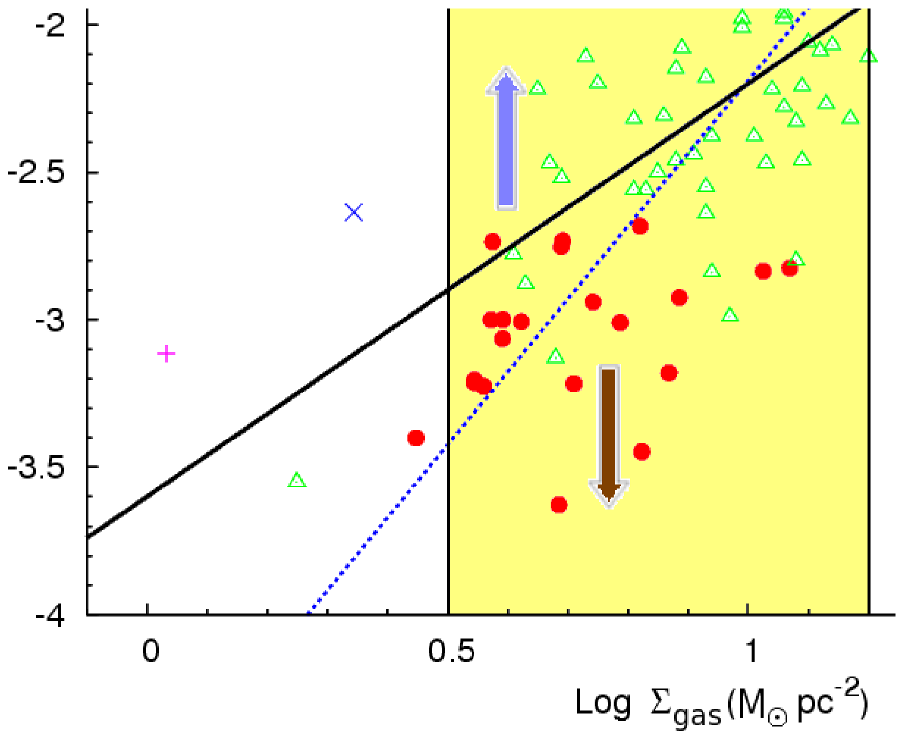

Caveats

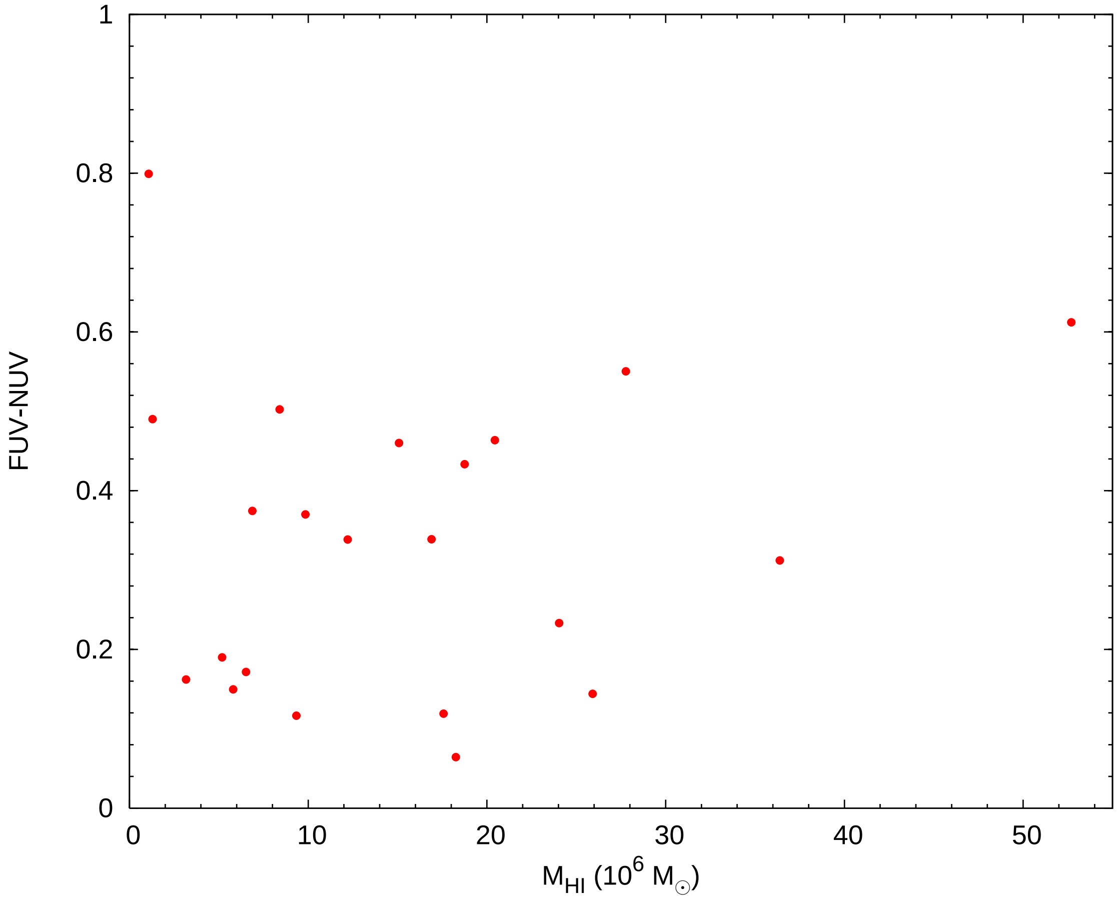

Disc averaged FUV-NUV colour of 22 galaxies, plotted against mass of HI gas contained within optical discs, having an average value of 0.34

Caveats

- According to Boissier et al. (2008), FUV-NUV color of 0.34 can result from the following models:
  - ▷ Galaxy has a Kroupa IMF with metallicity = $Z_\odot/20$, an age of 6.8×10^8 years, and star formation was quenched after 10^8 years
  - ▷ Has a Kroupa IMF truncated at $5M_\odot$ at the highend, solar metallicity, has been forming stars for 4.3×10^8 years continuously
  - ▷ Has an age of 2.4×10^8 years and star formation was quenched after 10^8 years
  - ▷ Has Kroupa IMF, solar metallicity, an age of 2.4×10^8 years and star formation was quenched after 10^8 years

Caveats

- Bigiel et al. (2008) did a similar study with THINGS galaxies, includes dwarfs, but pixel by pixel correlation not done for the four galaxies below the FIGGS magnitude limit
  - ▷ For the 4 irregular galaxies for which they do fit a power law, they find power law indices that vary from 1.59 to 2.78
  - ▷ They also find that the "star formation efficiency" (i.e. $\Sigma_{SFR}/\Sigma_{gas}$) is lower in dwarfs and the outer parts of spirals than in the inner, H_2 dominated regions of spiral galaxies
  - ▷ They also find that the gas density in dwarfs truncates sharply at about $9M_{\odot}/pc^2$ (study done at 750 pc linear resolution)

Caveats

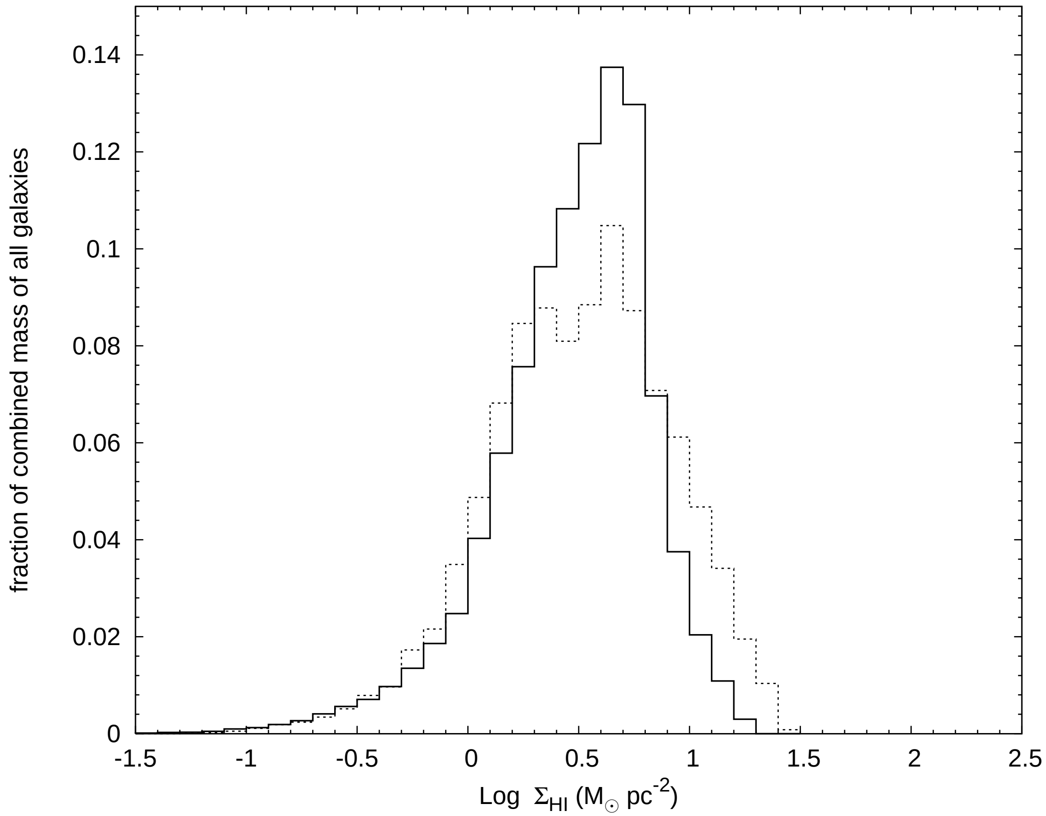

Histograms depicting what fraction of combined mass of all galaxies lie in a particular column density bin

- ⋆ Appears that HI gas occurs in small clumps whose density gets smoothed out when one observes with coarser resolution

MNRAS 397 1435-1453

Thank You